Self-Healing of Molecular Catalyst and Photosensitizer on Metal–Organic Framework: Robust Molecular System for Photocatalytic H_2 Evolution from Water

Dongha Kim, Dong Ryeol Whang,* and Soo Young Park*

Center for Supramolecular Optoelectronic Materials, Department of Materials Science and Engineering, Seoul National University, 1 Gwanak-ro, Gwanak-gu, Seoul 151-744, Korea

S *Supporting Information*

ABSTRACT: Inspired by self-repair mechanism of PSII in plants, we report a self-healing system which spontaneously repairs molecular catalyst and photosensitizer during photocatalytic H_2 evolution. A bipyridine-embedded UiO-type metal–organic framework (MOF), namely $Pt_n\_Ir\_BUiO$, which incorporated H_2-evolving catalyst and photosensitizer, was synthesized and subject to photocatalytic H_2 evolution reaction (HER). Impressively, HER with $Pt_{0.1}\_Ir\_BUiO$ showed very stable molecular photocatalysis without significant decrease in its activity and colloidal formation for 6.5 days at least; in the homogeneous counterpart, the molecular catalyst became a colloid just after 7.5 h. It was revealed that the arrangement of diimine sites which closely and densely surrounded the H_2-evolving catalyst and photosensitizer in the MOF enabled such a highly efficient self-healing.

In natural photosystem II (PSII), plants incorporate Mn-based molecular catalyst and chlorophyll within their lipid matrix for highly efficient solar-to-fuel conversion.[1] This principle has inspired artificial photosynthesis to use transition metal complexes as molecular catalysts and photosensitizers to mimic efficient charge transfer and solar-to-fuel conversion.[2] One implication is that the molecular catalysts are prone to undergo degradation in the photolysis conditions; more importantly, they sometimes act as precursors for colloidal metal catalysts.[3] Although colloidal catalysts, such as Pt or Pd colloid, often show high catalytic activities, they have intrinsic weak points in achieving tunability and selectivity. In this regard, preventing the transformation of molecular catalysts into metal colloids would be an important step toward artificial photosynthesis.

To circumvent the low stability of molecular catalysts and prevent unwanted transformation into metal colloids, using a self-healing platform that continuously repairs molecular catalysts would be a promising approach. Inspired by the self-repair mechanism of PSII in plants, Nocera et al. developed a heterogeneous cobalt catalyst which could repair itself with a phosphate counterion.[4] However, self-healing systems for molecular catalysts have not been carefully explored so far. The possibility of using a polymer system as a self-healing platform for molecular catalyst was proposed.[5] Eisenberg et al. reported regeneration of damaged molecular H_2-evolving catalyst by adding free ligand that reconstituted the catalyst.[6] Despite a few-fold increase in the catalyst's lifetime, the system was material-

Scheme 1. Schematic Operation Principle of Self-Healing MOF ($Pt_n\_Ir\_BUiO$) and the Corresponding Homogeneous System
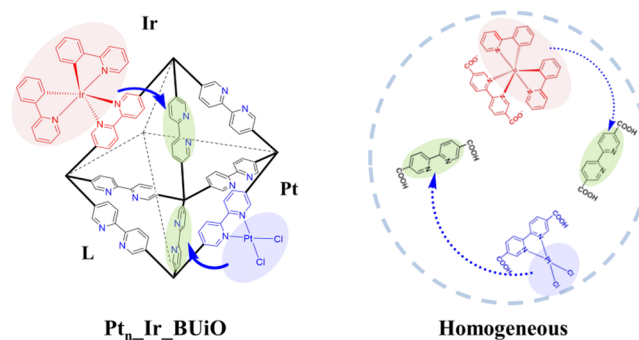
consuming and not sufficiently systematic to be termed as "self-healing".

To tackle the stability issue on molecular catalysts, there has been a way of confining them into heterogeneous systems such as inorganic nanoparticles and polymers.[7] Among those, metal–organic framework (MOF) has merits of high porosity and easy functionalization, and thus can provide unique means to engineer molecular catalysis in heterogeneous system.[8] Furthermore, integrating different functional units in MOF guarantees sufficient proximity between them to interact with each other for chemical reactions.[9] For example, molecular catalyst and photosensitizer were embedded in water-stable MOF and showed far more enhanced activity and stability in H_2 evolution reaction (HER) than the homogeneous counterpart.[10] Herein, we report an original strategy of using MOF as a self-healing system that not only supports HER but also spontaneously repairs embedded molecular catalyst and photosensitizer during the photocatalytic process. Water-stable bipyridine-embedded UiO-67 MOF, namely BUiO, was selected as a self-healing platform, and was functionalized with a molecular Pt(II) catalyst and an Ir(III) photosensitizer to yield $Pt_n\_Ir\_BUiO$ (Scheme 1). The reticular structure of the MOF arranged a number of diimine sites nearby the embedded transition metal complexes and facilitated rebonding of broken metal–diimine bonds during photocatalysis.
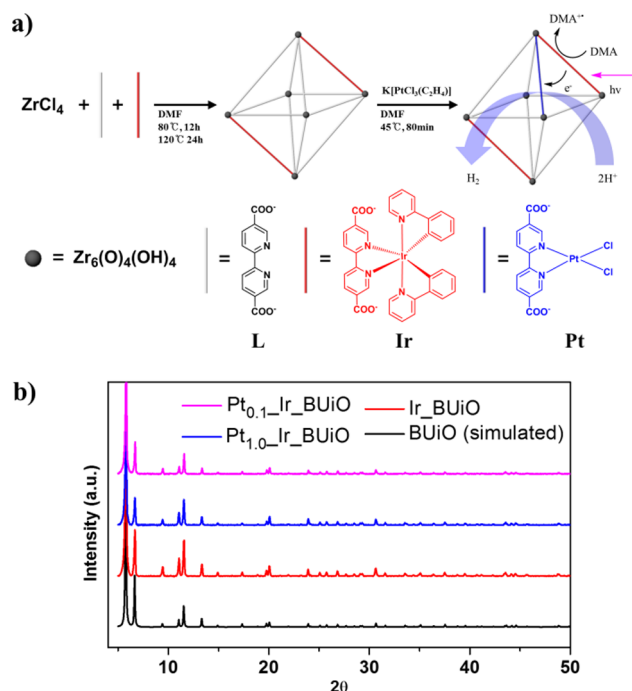
a)

b)

Figure 1. (a) Synthesis of Pt_n_Ir_BUiO and its photocatalytic mechanism. (b) PXRD patterns of $Pt_{0.1}$_Ir_BUiO (magenta), $Pt_{1.0}$_Ir_BUiO (blue), Ir_BUiO (red), and simulated BUiO (black).

As illustrated in Figure 1a, Pt_n_Ir_BUiO comprises 2,2′-bipyridine-5,5′-dicarboxylate (**L**) as a self-healing site, Pt^{II}(**L**)Cl_2 (**Pt**) as a H_2-evolving catalyst, and Ir^{III}(ppy)$_2$(**L**) (**Ir**) as a photosensitizer (ppy = phenylpyridine). As controls, a molecular catalyst, Pt^{II}(H_2**L**)Cl_2 (**H$_2$Pt**), and a photosensitizer, [Ir^{III}(ppy)$_2$(**L**)]$^-$Na$^+$ (**Na$^+$Ir**), were separately synthesized according to literature methods (H_2**L** is protonated **L**).[11] Three kinds of MOFs, $Pt_{0.1}$_Ir_BUiO, $Pt_{0.2}$_Ir_BUiO, and $Pt_{1.0}$_Ir_BUiO (the subscripts give the ratio of **Pt** to **Ir**), were synthesized by mixed-ligand synthesis and sequent post-synthetic metalation (PSM). As can be seen in Figure 1a, Ir_BUiO was first synthesized by treating a mixture of $ZrCl_4$, H_2**L**, and Na$^+$**Ir** under solvothermal condition. Next, **Pt** was incorporated in Ir_BUiO via PSM with varied feed amounts of Zeise's salt. Figure 1b shows that powder X-ray diffraction (PXRD) patterns of the MOFs were in accordance with BUiO single crystal (CCDC 968930), and the MOFs were highly porous in terms of BET areas (Supporting Information (SI), Figure S4). Successful PSM was supported by diffuse reflectance UV/vis spectra (SI, Figure S2). $Pt_{1.0}$_BUiO and $Pt_{0.1}$_BUiO showed prominent absorption peak at 418 nm which corresponds to metal-to-ligand ($Pt(d_\pi) \rightarrow$ dcbpy(π^*)) charge-transfer (MLCT) transition for H_2**Pt** in DMF.[10a] The Cl/Pt ratio was further quantified with energy-dispersive X-ray spectrometry (EDS) and inductively coupled plasma mass spectroscopy (ICP-MS) (SI, Figure S1 and Table S2). Additionally, the electron binding energies of Pt(II) $4f_{7/2}$ and $4f_{5/2}$ were very close to those in the analogous MOF (SI, Figure S5), and the Pt_n_Ir_BUiO suspension showed an orange to olive green color change after the beginning of photocatalysis, which is known to be observed when Pt(II)−diimine-type complexes are reduced (SI, Figure S6).[10a,12] The amount of each component in Pt_n_Ir_BUiO was determined by ICP-MS and ^{1}H NMR (SI, Figure S3), and field-emission scanning electron microscopy showed that the size of MOF particles ranged from 50 to 200 nm (SI, Figure S7).

In the case of Pt(II)−diimine complexes, the accessibility of the Pt(II) $d_{x^2−y^2}$ orbital upon two-electron reduction provides the main decomposition mechanism that breaks the Pt(II)−diimine bonds, and thus limits their molecular catalysis.[13] To examine whether H_2**Pt** would act as a molecular catalyst or just a precursor of Pt colloid, photocatalytic HER was carried out with H_2**Pt** and Na$^+$**Ir** in a homogeneous system. They were dissolved in a mixed solution of *N,N*-dimethylformamide (DMF):H_2O:*N,N*-dimethylaniline (DMA) (8:2:2 v/v/v), and the vial was continuously purged by 5 sccm of Ar. Using this continuous-flow system, we could calculate the H_2 evolution rate every 30 min with a gas chromatograph (see SI for experimental details). The sample was then irradiated with visible light from a xenon lamp with a 420 nm cutoff filter. The photocatalytic mechanism behind HER using DMA was examined by a quenching experiment, as described in Figure S8 (SI). It was revealed that the initial reaction with [Na$^+$**Ir**]* was a reductive quenching by electron transfer from DMA, not an oxidative one.[14] The reduced photosensitizer then transferred its excited electron to H_2**Pt** for H_2 evolution. Analogous reductive quenching mechanism of Ir(III) photosensitizer was also reported by Bernhard et al.[15] As a result of photocatalytic H_2 evolution, the sample showed fast saturating H_2 evolution curve; adding mercury, which can poison metal colloids, significantly attenuated the catalysis (Figure 2).
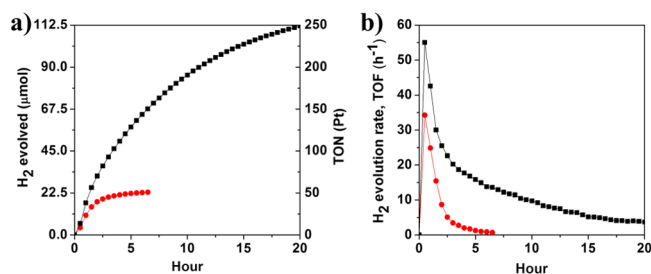
a)   **b)**

Figure 2. (a) H_2 evolution curve, i.e., amount of H_2 evolved vs time, of photocatalytic HER with 0.55 μmol of Na$^+$**Ir** and 0.45 μmol of H_2**Pt** (black), and the result of mercury poisoning experiment under the same conditions (red). (b) Corresponding H_2 evolution rate curve (black), turnover frequency (TOF) vs time, and the result of mercury poisoning (red).

As colloidal Pt formation is an autocatalytic reaction, which quickly consumes all available molecular Pt(II) complex in the system, it could be concluded that catalytically active Pt colloid was formed as soon as the reaction started.[16] In accordance with the previous study, this result indicated that H_2**Pt** was vulnerable under the photocatalytic conditions, and thus acted as a precursor of Pt colloid.[3d]

To circumvent the vulnerability of H_2**Pt** and prevent colloidal formation, 100 equiv of free H_2**L** ligand with respect to H_2**Pt** was added by referring to the strategy of Eisenberg.[6] We envisaged that when the Pt−diimine bond in H_2**Pt** was cleaved during HER, abundant H_2**L** ligand would promote re-coordination of Pt to its diimine site and recover the molecular catalytic activity of H_2**Pt**. Interestingly, three different catalytic behaviors in terms of H_2 evolution rate were observed during the photocatalysis (Figure 3a). Through mercury poisoning experiment, we assigned the stages as molecular catalysis (0−7.5 h), colloidal Pt formation (7.5−9 h), and colloidal catalysis (after 9 h). Importantly, the ratio of H_2**L** to H_2**Pt** was crucial in maintaining the molecular catalysis, as the time period of molecular catalysis was prolonged with increasing amount of H_2**L** (Figure 3b and SI,
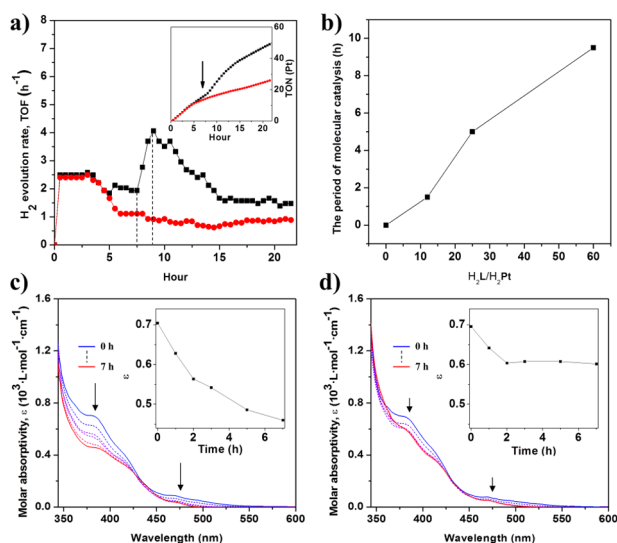
Figure 3. (a) H_2 evolution rate curve of photocatalysis driven with 0.30 μmol of Na^+Ir, 0.029 μmol of H_2Pt, and 3.0 μmol of H_2L (black), and the result of mercury poisoning experiment under the same conditions (red). Inset shows H_2 evolution curve, and arrow indicates the time colloidal formation began. (b) Duration of molecular catalysis with 0, 13, 25, and 60 equiv of H_2L per H_2Pt (with 0.55 μmol of Na^+Ir and 0.45 μmol of H_2Pt); TON = 0, 2.07, 10.0, and 16.5, respectively. UV/vis absorption change of Na^+Ir without (c) and with 13 equiv of H_2L (d) in a mixed solution of $DMF:H_2O:DMA$ (8:2:2 v/v/v). The sample was irradiated with visible light for 7 h. Insets show the change in the molar absorptivity of Na^+Ir at 380 nm.

Figure S9). This result was consistent with Eisenberg's experiment, in that an increased amount of ligand molecule extended the duration of molecular catalysis.[6a] In addition, Figure S9 shows that the maximum activity of colloidal catalysis decreases with increasing ratio of H_2L to H_2Pt. To examine the effect of H_2L on colloidal Pt formation, we added H_2L upon the formation of Pt colloid. As shown in Figure S10 (SI), H_2L affected colloidal Pt formation and reduced the maximum activity of Pt colloid. We concluded that adding H_2L affected the $Pt_n + nH_2L \rightleftarrows nPt-H_2L$ equilibrium and lowered the number of Pt colloids formed.[17] This effect became more influential with increasing amount of H_2L (SI, Figure S9). Additionally, it was previously reported by Bernhard et al. that the activity of a Pt colloid decreased when 2,2′-bipyridine, which is also one of diimines, was added at the beginning of photocatalysis.[15] Finally, to test the importance of diimine sites, 13 equiv of biphenyl-4,4′-dicarboxylic acid was added instead of H_2L, and only colloidal activity was observed without any repair of H_2Pt (SI, Figure S11).

Next, we examined whether free H_2L ligand would be also effective for recovery of Na^+Ir. It was reported that degradation of $[Ir^{III}(ppy)_2(bpy)]^+$ (bpy = bipyridine) photosensitizer during HER occurred mainly due to the cleavage of the Ir−diimine bond.[15] Hence, we prepared two batches of Na^+Ir solutions ($DMF:H_2O:DMA$ = 8:2:2 v/v/v), with and without 13 equiv of H_2L, and compared the changes in molar absorptivity (ε) of Na^+Ir upon degradation. Irradiation by visible light with a 420 nm cutoff filter reduced ε of Na^+Ir in both batches, but they showed differences after 2 h. Figure 3c shows that, in the batch without H_2L, ε continuously decreased during 7 h. However, in the batch with 13 equiv of H_2L, ε reached equilibrium after 2 h of irradiation, and there was no more degradation (Figure 3d). This result implies that Na^+Ir can be repaired by H_2L during

photocatalysis, and the strategy is effective for both H_2Pt and Na^+Ir.

To make a system that maximizes the repairing efficiency, we synthesized three bifunctional MOFs and investigated their photocatalytic behavior as self-healing systems. First, we conducted photocatalyis with $Pt_{0.1}$_Ir_BUiO under the same conditions as above homogeneous system. $Pt_{0.1}$_Ir_BUiO had an **L**-to-**Pt** ratio of 100, calculated from ^1H NMR and ICP-MS measurements. As a result, stable molecular catalysis was observed, recording $TON_{6.5\ days}$ = 343 and TOF_{max} = 2.9 h^{-1}, the highest TON among the systems using molecular Pt(II) catalysts (Figure 4).[2a,c,10a,c] High-resolution transmission elec-
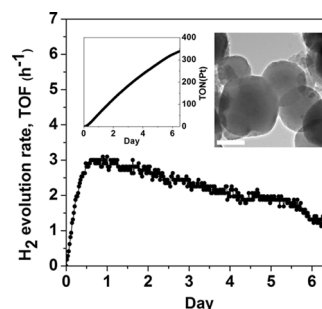

Figure 4. H_2 evolution rate curve of $Pt_{0.1}$_Ir_BUiO. The MOF contained 0.30 μmol of **Ir**, 0.029 μmol of **Pt**, and 3.0 μmol of **L**. Inset: H_2 evolution curve (left) and HR-TEM image of $Pt_{0.1}$_Ir_BUiO after 6.5 days (right, red square) of photocatalytic HER. Scale bar = 200 nm.

tron microscopy (HR-TEM) confirmed no trace of Pt colloid in $Pt_{0.1}$_Ir_BUiO, even after 6.5 days of photocatalytic HER (inset of Figure 4 and SI, Figure S12). We presumed that the initial induction period, in which the H_2 evolution rate gradually increased, was due to gas storage capacity of MOF, not colloidal Pt formation (see SI for detailed explanation). It is noteworthy that the molecular catalysis of $Pt_{0.1}$_Ir_BUiO lasted more than 6.5 days, while that of the control homogeneous system with the same amount of each species ceased after 7.5 h (SI, Table S3). The reason for such outstanding performance of the MOF system must have been the arrangement of diimine sites in the MOF, which closely and densely surrounded **Pt**. We also examined self-healing of **Ir** in MOF by comparing leaching amount of **Ir** from two different iridium-functionalized MOFs, Ir_BUiO and Ir_UiO, under the same photolysis condition ($DMF:H_2O:DMA$ = 8:2:2 v/v/v). In contrast to Ir_BUiO, Ir_UiO had biphenyl-4,4′-dicarboxylate as its linker without any free coordination site for self-healing. ICP-MS analysis showed that 0.90% and 4.0% of **Ir** was leached from each MOF after 1 day of visible light irradiation. In conjunction with the above degradation experiment in a homogeneous system, this significant difference in the leaching amounts of **Ir** indicated that the self-healing of **Ir** also operated in self-healing MOFs. Lastly, the amount of **Pt** and **Ir** leached from $Pt_{0.1}$_Ir_BUiO after 6 days of photocatalysis was found to be 7.8% and 2.4%, respectively. Also, PXRD data taken after 6 days of photocatalysis showed that the crystallinity of MOF was retained during the photocatalysis (SI, Figure S13). These results indicated that the photocatalysis was driven by catalytic species inside of $Pt_{0.1}$_Ir_BUiO, and the MOF was very stable in the meantime.

Next, MOFs with varied **L**-to-**Pt** ratios were subject to HER and their photocatalytic behaviors were investigated (Figure 5a and SI, Figure S14). Compared to the **L**-to-**Pt** ratio in $Pt_{0.1}$_Ir_BUiO, $Pt_{0.2}$_Ir_BUiO and $Pt_{1.0}$_Ir_BUiO had smaller
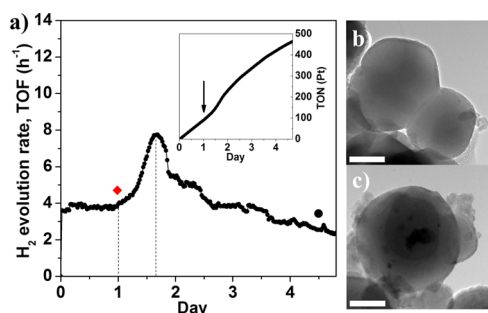
Figure 5. (a) H_2 evolution rate curve of $Pt_{1.0}$_Ir_BUiO showing three different catalytic behaviors: photocatalysis driven by molecular (first region), molecular + colloidal (second region), and colloidal (third region) catalyst. Inset: H_2 evolution curve of $Pt_{1.0}$_Ir_BUiO. (b,c) HR-TEM images of $Pt_{1.0}$_Ir_BUiO taken (b) after 1 day of photocatalytic HER, i.e., the red square in (a), and (c) after 5 days, i.e., the black circle in (a). Scale bar = 200 nm.

ratios of 62.5 and 10.0, respectively. $Pt_{1.0}$_Ir_BUiO showed molecular catalysis at the initial stage (0−1 day) and sequent colloidal formation (1−1.7 days), followed by colloidal catalysis after 1.7 days (Figure 5a). HR-TEM confirmed that there was no Pt colloid in the early stage (Figure 5b), which contrasted with the observation of several nanosized Pt colloids after 5 days (Figure 5c and SI, Figure S12). After the photocatalysis, the leaching amount of **Pt** and **Ir** from $Pt_{1.0}$_Ir_BUiO was calculated as 2.8% and 3.6%, respectively. Photocatalytic HER with $Pt_{0.2}$_Ir_BUiO also showed an intermediate self-healing period of 38 h (SI, Figures S14 and S15). This difference in the self-healing periods correlated well with the results in homogeneous systems, in which an increased H_2**L**-to-H_2**Pt** ratio extended the duration of molecular catalysis. Interestingly, the maximum colloidal activity of three self-healing MOFs showed a trend similar to that of homogeneous systems (SI, Figures S9 and S14). While three MOFs showed similar TOFs initially, they showed differences after 24 h ($Pt_{1.0}$_Ir_BUiO) and 38 h ($Pt_{0.2}$_Ir_BUiO). We believe that this is because the number of Pt colloids decreases with increasing **L**-to-**Pt** ratio in the MOF, just like in the homogeneous systems. In conclusion, the MOF systems are superior in self-healing compared to the homogeneous counterparts (SI, Table S3), and complete inhibition of colloidal formation can be established when sufficiently large **L**-to-**Pt** ratio is guaranteed in the MOF system.

In summary, integrating **Pt**, **Ir**, and **L** into UiO-67 MOF enabled self-healing of **Pt** and **Ir** during HER. We have demonstrated the principle of self-healing, its dependence on the ratio of **L** to **Pt**, and the superiority of a MOF system as a self-healing platform. The long-lasted debate on the fate of Pt(II) catalysts during photocatalysis (molecular or colloidal) is resolved in this work by clarifying the evolution of molecular Pt(II) catalyst to colloidal Pt catalyst.[2a,3b,d] Since many transition metal complexes are widely used in various photocatalyses, we believe that our novel strategy of using a self-healing MOF platform will pave the way for making highly stable photocatalytic systems.

■ ASSOCIATED CONTENT

Ⓢ Supporting Information

The Supporting Information is available free of charge on the ACS Publications website at DOI: 10.1021/jacs.6b04552.

　　Experimental details, synthesis, and additional characterization of MOF systems (PDF)

■ AUTHOR INFORMATION

Corresponding Author

*pippop@snu.ac.kr; parksy@snu.ac.kr

Notes

The authors declare no competing financial interest.

■ REFERENCES

(1) Umena, Y.; Kawakami, K.; Shen, J. R.; Kamiya, N. *Nature* **2011**, *473*, 55.

(2) (a) Ozawa, H.; Sakai, K. *Chem. Commun.* **2011**, *47*, 2227. (b) Stoll, T.; Gennari, M.; Fortage, J.; Castillo, C. E.; Rebarz, M.; Sliwa, M.; Poizat, O.; Odobel, F.; Deronzier, A.; Collomb, M. N. *Angew. Chem.* **2014**, *126*, 1680. (c) Knoll, J. D.; Arachchige, S. M.; Brewer, K. J. *ChemSusChem* **2011**, *4*, 252.

(3) (a) Artero, V.; Fontecave, M. *Chem. Soc. Rev.* **2013**, *42*, 2338. (b) Eckenhoff, W. T.; Eisenberg, R. *Dalton Trans.* **2012**, *41*, 13004. (c) Pfeffer, M. G.; Schafer, B.; Smolentsev, G.; Uhlig, J.; Nazarenko, E.; Guthmuller, J.; Kuhnt, C.; Wachtler, M.; Dietzek, B.; Sundstrom, V.; Rau, S. *Angew. Chem. Int. Ed.* **2015**, *54*, 5044. (d) Du, P.; Schneider, J.; Li, F.; Zhao, W.; Patel, U.; Castellano, F. N.; Eisenberg, R. *J. Am. Chem. Soc.* **2008**, *130*, 5056.

(4) Lutterman, D. A.; Surendranath, Y.; Nocera, D. G. *J. Am. Chem. Soc.* **2009**, *131*, 3838.

(5) Krawicz, A.; Yang, J.; Anzenberg, E.; Yano, J.; Sharp, I. D.; Moore, G. F. *J. Am. Chem. Soc.* **2013**, *135*, 11861.

(6) (a) Lazarides, T.; McCormick, T.; Du, P. W.; Luo, G. G.; Lindley, B.; Eisenberg, R. *J. Am. Chem. Soc.* **2009**, *131*, 9192. (b) McCormick, T. M.; Han, Z.; Weinberg, D. J.; Brennessel, W. W.; Holland, P. L.; Eisenberg, R. *Inorg. Chem.* **2011**, *50*, 10660.

(7) Yagi, M.; Kaneko, M. *Chem. Rev.* **2001**, *101*, 21.

(8) (a) Manna, K.; Zhang, T.; Lin, W. *J. Am. Chem. Soc.* **2014**, *136*, 6566. (b) Manna, K.; Zhang, T.; Greene, F. X.; Lin, W. *J. Am. Chem. Soc.* **2015**, *137*, 2665. (c) Falkowski, J. M.; Sawano, T.; Zhang, T.; Tsun, G.; Chen, Y.; Lockard, J. V.; Lin, W. *J. Am. Chem. Soc.* **2014**, *136*, 5213. (d) Fei, H.; Cohen, S. M. *J. Am. Chem. Soc.* **2015**, *137*, 2191. (e) Fei, H.; Shin, J.; Meng, Y. S.; Adelhardt, M.; Sutter, J.; Meyer, K.; Cohen, S. M. *J. Am. Chem. Soc.* **2014**, *136*, 4965.

(9) (a) Wang, C.; deKrafft, K. E.; Lin, W. *J. Am. Chem. Soc.* **2012**, *134*, 7211. (b) Zhang, Z. M.; Zhang, T.; Wang, C.; Lin, Z.; Long, S.; Lin, W. *J. Am. Chem. Soc.* **2015**, *137*, 3197. (c) Maza, W. A.; Padilla, R.; Morris, A. J. *J. Am. Chem. Soc.* **2015**, *137*, 8161.

(10) (a) Hou, C.-C.; Li, T.-T.; Cao, S.; Chen, Y.; Fu, W.-F. *J. Mater. Chem. A* **2015**, *3*, 10386. (b) Pullen, S.; Fei, H.; Orthaber, A.; Cohen, S. M.; Ott, S. *J. Am. Chem. Soc.* **2013**, *135*, 16997. (c) Zhou, T.; Du, Y.; Borgna, A.; Hong, J.; Wang, Y.; Han, J.; Zhang, W.; Xu, R. *Energy Environ. Sci.* **2013**, *6*, 3229.

(11) (a) Szeto, K. C.; Kongshaug, K. O.; Jakobsen, S.; Tilset, M.; Lillerud, K. P. *Dalton Trans.* **2008**, *15*, 2054. (b) Tamayo, A. B.; Alleyne, B. D.; Djurovich, P. I.; Lamansky, S.; Tsyba, I.; Ho, N. N.; Bau, R.; Thompson, M. E. *J. Am. Chem. Soc.* **2003**, *125*, 7377.

(12) Collison, D.; Mabbs, F. E.; McInnes, E. J. L.; Taylor, K. J.; Welch, A. J.; Yellowlees, L. J. *J. Chem. Soc., Dalton Trans.* **1996**, 329.

(13) Whang, D. R.; Park, S. Y. *ChemSusChem* **2015**, *8*, 3204.

(14) *Proceedings of the Seventh International Symposium on the Photochemistry and Photophysics of Coordination Compounds*; Yersin, H., Vogler, A., Eds.; Springer-Verlag: Berlin, 1987; p 144.

(15) Tinker, L. L.; McDaniel, N. D.; Curtin, P. N.; Smith, C. K.; Ireland, M. J.; Bernhard, S. *Chem. - Eur. J.* **2007**, *13*, 8726.

(16) Besson, C.; Finney, E. E.; Finke, R. G. *J. Am. Chem. Soc.* **2005**, *127*, 8179.

(17) Widegren, J. A.; Finke, R. G. *J. Mol. Catal. A: Chem.* **2003**, *198*, 317.